

# Vibroacoustic Response of Flexible Car Components

J. Herrmann<sup>1</sup>, M. Junge<sup>1</sup> and L. Gaul<sup>1</sup>

**Abstract:** The influence of an acoustic field on the dynamic behavior of a flexible structure is a common issue in automotive applications. An example is the pressure-induced structure-borne sound of piping and exhaust systems. Efficient model order reduction and substructuring techniques accelerate the finite element analysis and enable the vibroacoustic optimization of such complex systems with acoustic fluid-structure interaction. This research reviews the application of the Craig-Bampton and the Rubin method to fluid-structure coupled systems and presents two automotive applications. First, a fluid-filled piping system is assembled by substructures or superelements according to the Craig-Bampton method. Fluid and structural partitions are fully coupled in order to capture the interaction between the pipe shell and the heavy fluid inside the pipe. Moreover, a fluid-filled corrugated pipe is efficiently modeled and analyzed. Second, a rear muffler with an air-borne excitation is investigated. Here, the Rubin and the Craig-Bampton method are used to separately compute the uncoupled component modes of both the acoustic and the structural domain. These modes are then used to compute a reduced model that incorporates full acoustic-structure coupling. For both applications, transfer functions are computed and compared to the results of dynamic measurements.

**Keywords:** acoustic fluid-structure interaction, FEM, substructuring, model reduction, dynamic measurements.

## 1 Introduction

Flexible piping and exhaust systems are often excited by (hydro-)acoustic sources. An example for a hydroacoustic excitation in hydraulic pipes such as fuel and brake pipes is the operation of pumps and hydraulic valves which leads to oscillating pressure pulsations within the pipe. As a result, pressure waves propagate along the pipe and excite the pipe shell due to heavy fluid-structure coupling [Maess

---

<sup>1</sup> Institute of Applied and Experimental Mechanics, University of Stuttgart, Pfaffenwaldring 9, 70550 Stuttgart.

(2006); Herrmann (2011)]. Finally, the pressure-induced structure-borne sound is transmitted to attached structures which leads to undesired noise and vibration levels. A similar excitation scenario is found in automotive exhaust systems where the exhaust gas acts as a strong acoustic source which also leads to pressure-induced structure-borne sound and undesired sound radiation [Junge (2010)].

To predict the vibroacoustic behavior of such mechanical systems, three-dimensional models including full coupling of the two-field problem are needed. It is particularly important to include bending modes of the structure, which are predominantly responsible for sound and vibration harshness. The finite element method [Zienkiewicz and Taylor (2000)] is considered as the appropriate discretization method to investigate the dynamics of the interior vibroacoustic problem including the coupling between the inner fluid and the pipe shell. The boundary element method might be used to determine the sound radiation in the exterior field [Gaul, Kögel, and Wagner (2003); Brunner, Junge, and Gaul (2009)].

The main problem of fully discretized models are large computation times and extensive computer memory. Model order reduction and substructuring techniques such as the well-known component mode synthesis overcome this limitation [de Klerk, Rixen, and Voormeeren (2008)]. This research shows how the Craig-Bampton and the Rubin method [Craig and Bampton (1968); Rubin (1975)] are applied to efficiently compute the hydro- and vibroacoustic response of typical automotive applications. First, fluid-filled piping systems are analyzed which are characterized by a heavy fluid-structure coupling between the fluid inside the pipe and the flexible pipe shell. Second, an automotive exhaust system is analyzed, which is an example of light fluid-structure coupling between the exhaust gas and the structure of the expansion chamber. Here, the Rubin and the Craig-Bampton method are used to separately determine the uncoupled component modes of both the acoustic and the structural domain. These modes are then used to compute a reduced model including full acoustic-structure coupling. Measurements are performed and the vibroacoustic response is compared to the results of the numerical simulation including the proposed model reduction technique. For all described applications, dynamic measurements are conducted on realistic test benches and the vibroacoustic response is compared to the results of the numerical simulation.

This invited paper summarizes the results and conclusions of our previous publications about automotive piping and exhaust systems [Maess and Gaul (2006); Herrmann, Maess, and Gaul (2010); Junge, Brunner, Walz, and Gaul (2010)] and may serve as a guideline for the efficient solution of industrial vibroacoustic problems.

## 2 Finite Element Based Substructuring Techniques Applied to Vibroacoustic Problems

This chapter briefly summarizes the application of the Craig-Bampton and the Rubin method on fluid-structure coupled systems. Both methods are used to reduce the order of the corresponding finite element model of each component and to assemble the overall mechanical system.

The acoustic domain is described by the linear wave equation without superimposed mean flow. This approach is valid for low Mach numbers as encountered in most piping and exhaust systems [Maess (2006)]. Acoustic fluid-structure coupling is present at the fluid-structure interface, where two coupling conditions hold, namely the continuity of particle velocities as well as the equilibrium of reaction forces. The corresponding finite element formulation leads to coupled discretized equations in terms of nodal structural displacements  $u$  and nodal acoustic excess pressures  $p$  [Zienkiewicz and Taylor (2000)]

$$\begin{bmatrix} M_s & 0 \\ \rho_0 C^T & M_a \end{bmatrix} \begin{bmatrix} \ddot{u} \\ \ddot{p} \end{bmatrix} + \begin{bmatrix} D_s & 0 \\ 0 & D_a \end{bmatrix} \begin{bmatrix} \dot{u} \\ \dot{p} \end{bmatrix} + \begin{bmatrix} K_s & -C \\ 0 & K_a \end{bmatrix} \begin{bmatrix} u \\ p \end{bmatrix} = \begin{bmatrix} f(t) \\ q(t) \end{bmatrix}. \quad (1)$$

In the above equations, index “s” denotes the structure, whereas index “a” characterizes the acoustic fluid. The system matrices of the structure are given by  $M_s$  and  $K_s$ , whereas the corresponding acoustic system matrices are defined as  $M_a$  and  $K_a$ . The viscous damping matrices are written as  $D_{s,a}$  and the coupling matrix is denoted by  $C$ . Forces and fluxes are given by  $f(t)$  and  $q(t)$ . Hereby, the classical unsymmetric formulation with displacements and pressures as field variables is used. It is worth noting that alternative representations use the acoustic velocity potential as field variable [Everstine (1981)] which leads to a symmetric formulation of Eq. (1). Another interesting approach is the symmetrization of Eq. (1) using appropriate scaling matrices as suggested by Felippa (1985).

### 2.1 Craig-Bampton Method

The adaptation of the Craig-Bampton method to mechanical systems with acoustic fluid-structure coupling has been developed in [Maess and Gaul (2006)]. For clarity, the critical steps are briefly summarized in this section. To apply the Craig-Bampton method to the acoustic-structure coupled problem, displacement and pressure DOFs are separated in interface DOFs with index “I” and inner/free DOFs denoted by index “F”. The matrices are partitioned accordingly. The Craig-Bampton reduction basis consists of fixed interface modes and constraint modes [Craig and

Bampton (1968)]. The fixed interface modes are obtained by solving the coupled eigenvalue problem for the system with constrained interface DOFs

$$\left( \begin{bmatrix} K_{s,FF} & -C_{FF} \\ 0 & K_{a,FF} \end{bmatrix} - \omega_j^2 \begin{bmatrix} M_{s,FF} & 0 \\ \rho_0 C_{FF}^T & M_{a,FF} \end{bmatrix} \right) \begin{bmatrix} \hat{u}_{j,F} \\ \hat{p}_{j,F} \end{bmatrix} = 0. \tag{2}$$

The reduction bases  $\Phi$  are enriched by a sufficient number of fixed interface modes. In many applications, the number of fixed interface modes is controlled by a frequency threshold that is usually at least two times the maximum frequency of interest. A modification of an iterative subspace solver is applied to compute the eigenvectors [Bobillot and Balmès (2002); Maess (2006)]. The constraint modes  $\Psi$  follow from a static of Guyan condensation [Guyan (1965)]. In this research, the constraint modes are computed by discarding fluid-structure coupling terms. One has to keep in mind that the acoustic rigid body mode is no longer solution of the reduced problem if the constraint modes are computed without coupling terms. As described by [Ohayon (2004)], the influence of the static deformation of the pipe structure has to be taken into account to obtain the correct static pressure.

The resulting reduction bases  $\Gamma_s$  and  $\Gamma_a$  are given by

$$\begin{bmatrix} u_I \\ u_F \end{bmatrix} = \begin{bmatrix} I & 0 \\ -K_{s,FF}^{-1}K_{s,FI} & \Phi_{s,FF} \end{bmatrix} \begin{bmatrix} u_I \\ \eta_s \end{bmatrix} = [ \Psi_s \quad \Phi_s ] q_s = \Gamma_s q_s \tag{3}$$

for the structural domain and

$$\begin{bmatrix} p_I \\ p_F \end{bmatrix} = \begin{bmatrix} I & 0 \\ -K_{a,FF}^{-1}K_{a,FI} & \Phi_{a,FF} \end{bmatrix} \begin{bmatrix} p_I \\ \eta_a \end{bmatrix} = [ \Psi_a \quad \Phi_a ] q_a = \Gamma_a q_a \tag{4}$$

for the fluid domain, respectively. The modal coordinates  $\eta$  are associated to dominant fixed interface modes that are retained. Higher frequency normal modes are truncated. Hence,  $q_s$  and  $q_a$  are the generalized coordinates of the reduced system. The overall reduction basis is assembled by

$$\begin{bmatrix} u \\ p \end{bmatrix} = \underbrace{\begin{bmatrix} \Gamma_s & 0 \\ 0 & \Gamma_a \end{bmatrix}}_{\Gamma \in \mathbb{R}^{n \times n_r}} \begin{bmatrix} q_s \\ q_a \end{bmatrix} \tag{5}$$

and reduces the coupled system in Eq. (1) to  $n_r \ll n$  DOFs

$$\begin{bmatrix} M_s^\diamond & 0 \\ \rho_0 C^{\diamond T} & M_a^\diamond \end{bmatrix} \begin{bmatrix} \ddot{q}_s \\ \ddot{q}_a \end{bmatrix} + \begin{bmatrix} K_s^\diamond & -C^\diamond \\ 0 & K_a^\diamond \end{bmatrix} \begin{bmatrix} q_s \\ q_a \end{bmatrix} = \begin{bmatrix} f_s \\ f_a \end{bmatrix} \tag{6}$$

where

$$\begin{aligned} M_s^\diamond &= \Gamma_s^T M_s \Gamma_s, & M_a^\diamond &= \Gamma_a^T M_a \Gamma_a, & K_s^\diamond &= \Gamma_s^T K_s \Gamma_s, & K_a^\diamond &= \Gamma_a^T K_a \Gamma_a, \\ C^\diamond &= \Gamma_a^T C \Gamma_s, & f_s &= \Gamma_s^T f & f_a &= \Gamma_a^T q. \end{aligned} \quad (7)$$

Eq. (6) defines one specific superelement for the component mode synthesis. It is important to note that both structural and fluid interface DOFs are kept as physical DOFs which simplifies the component coupling procedure and which allows the integration of Dirichlet and impedance boundary conditions in the reduced equations. The Craig-Bampton method is particularly efficient for piping systems, where the number of interface DOFs between the components is small compared to the inner DOFs and where repeating superelements occur. An additional reduction of the remaining interface DOFs leads to a further computational speedup and may be applied as explained in [Herrmann, Maess, and Gaul (2010); Junge, Brunner, Becker, and Gaul (2009)]. The described component model reduction is realized without consideration of damping. However, viscous damping models are integrated in the global dynamic equations in a subsequent step as described later in this section.

The coupling between reduced component models is realized by applying Lagrange's equations with Lagrange multipliers. The first way to assemble substructures is the elimination of the Lagrange multipliers using an appropriate transformation or coupling matrix (denoted as  $Q$  in this article) to transform the component coordinates in coordinates of the assembled piping system. This approach, often called primal assembly, is applied in this research to ensure rigid coupling of  $n_{\text{sub}}$  substructure contributions. A second way to assemble components is the so-called dual substructure assembly, where the Lagrange multipliers remain as additional degrees of freedom [Rixen (2004); de Klerk, Rixen, and Voormeeren (2008)].

The global dynamic system of equations with the global reduced coordinates  $q = [q_s \ q_a]^T$  is given by

$$M_g \ddot{q} + D_g \dot{q} + K_g q = f_g, \quad (8)$$

whereas the system matrices  $M_g$  and  $K_g$  are assembled as

$$M_g = \sum_{i=1}^{n_{\text{sub}}} \begin{bmatrix} Q_{s,i}^T M_{s,i}^\diamond Q_{s,i} & 0 \\ \rho_0 Q_{a,i}^T C_i^\diamond Q_{s,i} & Q_{a,i}^T M_{a,i}^\diamond Q_{a,i} \end{bmatrix}, \quad (9)$$

$$K_g = \sum_{i=1}^{n_{\text{sub}}} \begin{bmatrix} Q_{s,i}^T K_{s,i}^\diamond Q_{s,i} & -Q_{s,i}^T C_i^\diamond Q_{a,i} \\ 0 & Q_{a,i}^T K_{a,i}^\diamond Q_{a,i} \end{bmatrix}. \quad (10)$$

The global forces and fluxes are assembled accordingly. The global viscous damping matrix is given by

$$D_g = \sum_{i=1}^{n_{sub}} \begin{bmatrix} \alpha_{s,i} Q_{s,i}^T M_{s,i}^\diamond Q_{s,i} + \beta_{s,i} Q_{s,i}^T K_{s,i}^\diamond Q_{s,i} & 0 \\ 0 & \beta_{a,i} Q_{a,i}^T K_{a,i}^\diamond Q_{a,i} \end{bmatrix}, \quad (11)$$

assuming a Rayleigh damping model for each substructure with the corresponding Rayleigh damping parameters  $\alpha_s$  and  $\beta_s$  for the structural domain and  $\beta_a$  for the fluid partition. With this simplified approach, the influence of damping is captured in a post-processing step and the computation of complex component modes is avoided. For fluid-filled pipes, a considerable improvement of the fluid damping model is achieved using an advanced modeling approach including wall friction effects that is the dominant damping mechanism in thin pipes [Tijdeman (1975)]. The advanced fluid damping model is based on a complex wave number and incorporates the frequency dependent wall friction between the acoustic fluid and the pipe shell. The integration of this improved fluid damping model in the finite element analysis is explained in [Herrmann, Koreck, Maess, Gaul, and von Estorff (2011)].

In the frequency domain, Eq. (8) is given by

$$(-M_g \omega^2 + i\omega D_g + K_g) \hat{q} = \hat{f}_g, \quad (12)$$

such that a harmonic analysis is performed using the inverse of the dynamic stiffness matrix as transfer function. The results are expanded to full space in order to obtain the transfer function of interest.

## 2.2 Rubin Method

In contrast to the Craig-Bampton method, the Rubin method is a free-interface method, i.e. neither the interface DOFs nor the free DOFs are additionally constrained for the computation of the component modes in  $\hat{\Gamma}$ , which is assembled by free-interface normal modes and attachment modes [Rubin (1975)]. In what follows, the basic principle of the Rubin method is explained on behalf of the structural domain.

The free-interface normal modes are computed by solving the eigenvalue problem of the unconstrained system

$$(-\omega_j^2 M_s + K_s) \hat{\Phi}_{s,j} = 0. \quad (13)$$

Analogue to the Craig-Bampton method, only a small number of free-interface normal modes are retained. Attachment modes,  $\hat{\Psi}_s$ , augment the component modes matrix accounting for the modal truncation error. The  $i$ -th attachment mode is

defined by the static solution vector due to a single unit force applied to the  $i$ -th interface DOF

$$\hat{\Psi}_{si} = \begin{bmatrix} K_{s,\Pi} & K_{s,IF} \\ K_{s,FI} & K_{s,FF} \end{bmatrix}^{-1} [0 \quad \dots \quad 1 \quad \dots \quad 0]^T . \tag{14}$$

In other words, attachment modes are columns of the associated flexibility matrix. The reduction basis  $\hat{\Gamma}$  is then given by

$$\hat{\Gamma}_s = [\hat{\Psi}_s \quad \hat{\Phi}_s] . \tag{15}$$

Attachment modes cannot be computed directly, if the structure possesses rigid body degrees of freedom. Then, instead of the standard attachment modes, inertia-relief attachment modes represent one alternative [Craig Jr. (2000)].

The coupling between the reduced component models is analogue to the Craig-Bampton method. Since for the Craig-Bampton method all interface DOFs are retained, the displacement coupling conditions are typically fulfilled more accurately than with the Rubin method. Yet, if experimentally determined modal damping ratios are to be incorporated in the simulation model, the Rubin method is favorable. The free-floating boundary conditions of the free-interface normal modes can be realized in an experimental setup. Thus, the obtained modal damping ratios may be mapped directly.

### 2.3 Combination of Craig-Bampton and Rubin Method for Light Fluid-Structure Coupling

It is observed that for structures with high impedance mismatch between the structure and the contained fluid, the coupled eigenfrequencies and eigenvectors are altered only marginally compared to the uncoupled ones. Therefore, in such a case, the reduced-order model is constructed by using the uncoupled eigenvectors, since they span approximately the same subspace as the coupled eigenvectors. This is equivalent to reducing each domain separately. Please note that the reduced-order model is still a fully coupled system. This approach has the advantage that for each domain the favorable reduction method may be applied. If for example the Rubin method is applied for the reduction of the structure and the Craig-Bampton method is used for the fluid, the reduction basis reads

$$\hat{\Gamma} = \begin{pmatrix} \hat{\Psi}_s & \hat{\Phi}_s & 0 & 0 \\ 0 & 0 & \Psi_a & \Phi_a \end{pmatrix} . \tag{16}$$

Note that all component mode vectors in  $\hat{\Gamma}$  are obtained by the solution of the uncoupled problem.

### 3 Applications

So far, the application of substructuring techniques to problems with acoustic-structure coupling has been elaborated. Now, typical industrial applications are presented, where the different model reduction techniques are applied.

#### 3.1 Vibroacoustic Analysis of an Elbow Piping System

The focus of this section is the hydro- and vibro-acoustic analysis of thin piping systems (e.g. automotive brake and fuel pipes). The first example is a fluid-filled elbow piping system which is characterized by a heavy fluid-structure coupling between the fluid inside the pipe and the flexible shell. The piping system consists of a curved brake pipe (lengths 0.7 m + 0.3 m) with an outer radius of 3 mm and a wall thickness of 0.7 mm, two steel joints (the so-called clips) and a plate as target structure (lengths 0.3 m x 0.3 m x 0.001 m). The pipe is filled with water. The investigated pipe configuration is of practical importance since pressure pulsations in the fluid and strong fluid-structure coupling result in a considerable structural excitation of the brake pipe. The pressure-induced structure-borne sound is transferred to the target structure by the clips as explained in [Herrmann (2011)]. The Craig-

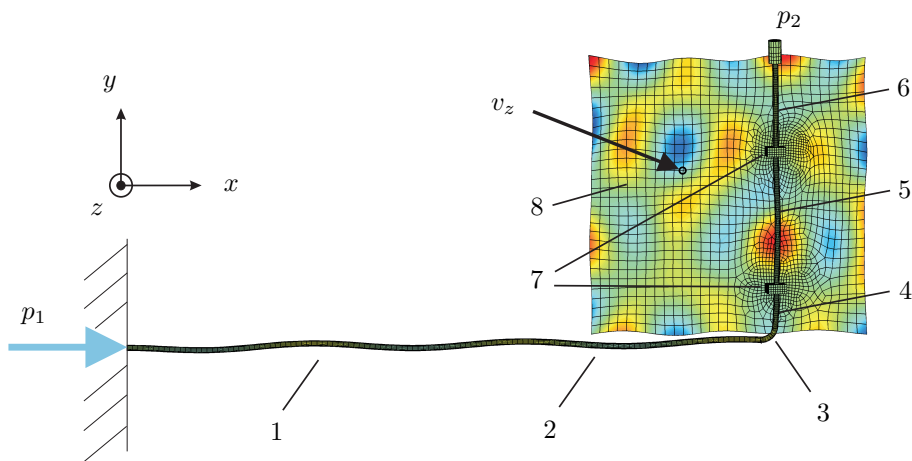


Figure 1: Assembled brake-pipe system after dynamic substructuring.

Bampton method is used as dynamic substructuring technique to assemble the piping system. Fig. 1 shows the pipe configuration assembled by 9 substructures (five straight pipe sections, one elbow, two clips and the plate). The application of the Craig-Bampton method reduces the model order from 55818 DOFs to 2566 DOFs.

The additional interface reduction as introduced in [Herrmann, Maess, and Gaul (2010)] leads to 1118 DOFs.

The experimental setup of the hydraulic test bench is illustrated in Fig. 2 and is also described in [Herrmann, Maess, and Gaul (2010); Herrmann, Haag, Gaul, Bendel, and Horst (2008)]. The setup consists of a hydroacoustic pressure source and a fluid-filled piping system with the dimensions mentioned before. The pressure source generates pressure pulsations in the fluid column. The supply pipe with the additional pump is required to fill and compress the fluid to ensure a stable fluid column without any air bubbles. The dynamic pressure pulsations are measured with piezoelectric pressure sensors. A sweep excitation is chosen in order to excite a wide frequency range. Averaged auto-power and cross-power spectra are finally used to estimate hydraulic and vibroacoustic transfer functions. To validate

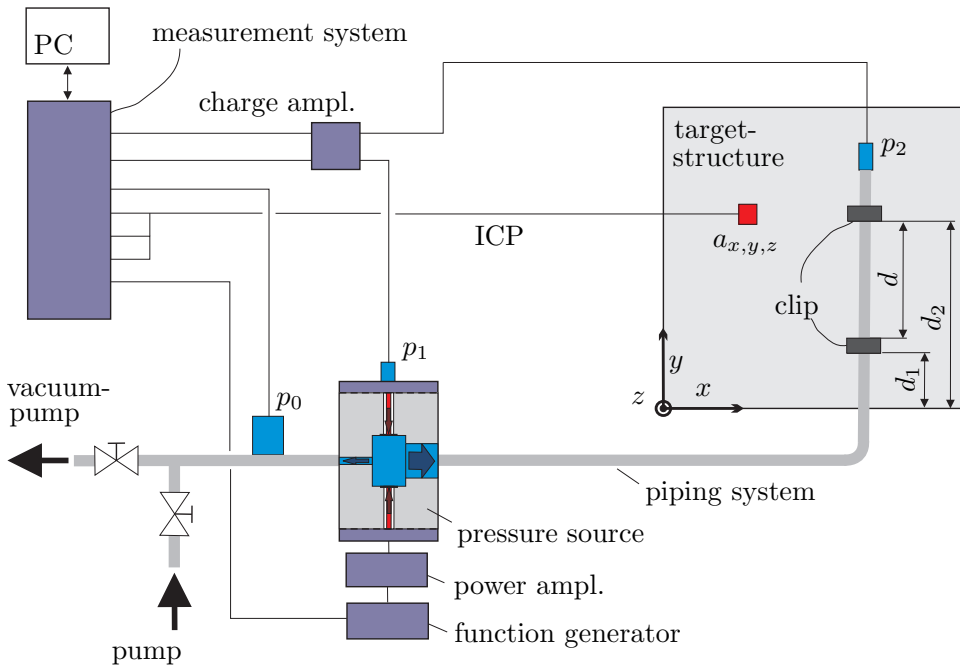


Figure 2: Experimental setup of the hydraulic test bench including pressure source.

the overall simulation method, the measured and the computed transfer functions are compared in Fig. 3. Both, the vibroacoustic transfer function between the input pressure and the normal velocity of a representative measurement point on the target structure,  $H_{p_1 \rightarrow v_z}$ , and the hydraulic transfer function,  $H_{p_1 \rightarrow p_2}$ , are depicted in Fig. 3. The transfer functions are denoted as  $H_{input \rightarrow output}$ . The unit of the vi-

broacoustic FRF is  $\frac{\text{m}^3}{\text{Ns}}$ . However, the magnitude of the FRF is depicted in dB with respect to the reference of  $1 \frac{\text{m}^3}{\text{Ns}}$ . The correlation between dynamic measurement and simulation is quite promising, particularly for the hydraulic transfer function. The magnitude of the vibroacoustic transfer function reveals many resonance peaks due to the high modal density of the thin target structure. This makes the correlation between experiment and simulation difficult. However, the overall amplitude level shows a reasonable correspondence. At the hydraulic resonances, the measured and the computed magnitude of the vibroacoustic transfer function match quite well. Strong acoustic-structure coupling is observed for a frequency around 1800 Hz, where a hydraulic and a structural resonance coincide. The resulting resonances are located at modified frequencies compared to the uncoupled system. It turns out that this coupled mode is very sensitive with respect to the structural configuration and the pipe mounting position.

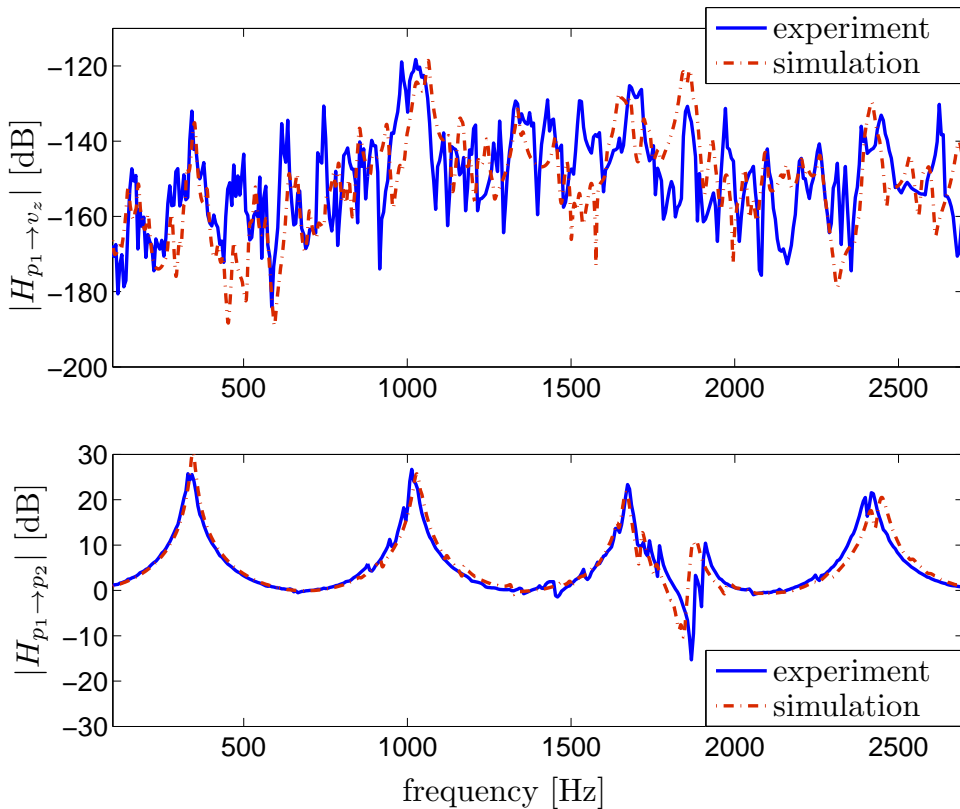


Figure 3: Top: magnitude of vibroacoustic transfer function. Bottom: magnitude of hydraulic transfer function.

### 3.2 Vibroacoustic Analysis of Corrugated Pipes

Corrugated pipes are characterized by a strong interaction of the pipe structure with the acoustic fluid. For instance, the fluid wave speed is significantly altered by a corrugated pipe structure [Maess, Herrmann, and Gaul (2007)]. The investigated corrugated hose is attached to the previously described pulsation source as depicted in Fig. 4. Furthermore, the displacement of the free end of the hose is measured

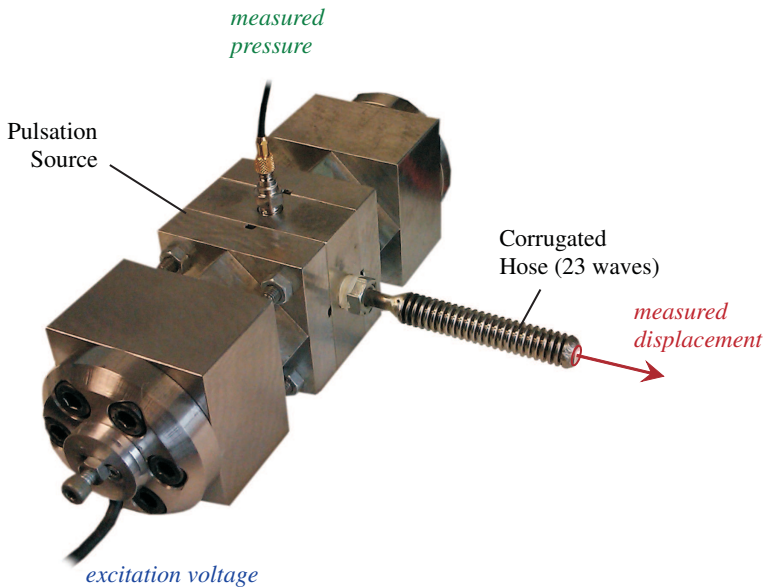


Figure 4: Corrugated hose attached to pulsation source for dynamic pressure loads.

with a Laser Doppler Vibrometer. The measured transfer function of the input voltage to the dynamic pressure at the pipe inlet as well as the transfer function of the input voltage to the longitudinal displacement at the end of the pipe are shown in Fig. 5. The observed resonances are caused by the coupled system of the interior fluid domain and the dynamic behavior of the hose structure. With this setup, it is possible to analyze the dependency between pressure amplitudes and hose deformation.

Of course, the previously described dynamic substructuring methods may be applied to analyze the vibroacoustic response of the interior pipe problem. If the pipe engineer is rather interested in the free wave characteristics of the complete waveguide, it is rather recommended to use the so-called waveguide finite element method as developed by [Mace, Duhamel, Brennan, and Hinke (2005)] and applied to fluid-filled corrugated piping systems by [Maess, Herrmann, and Gaul (2007)].

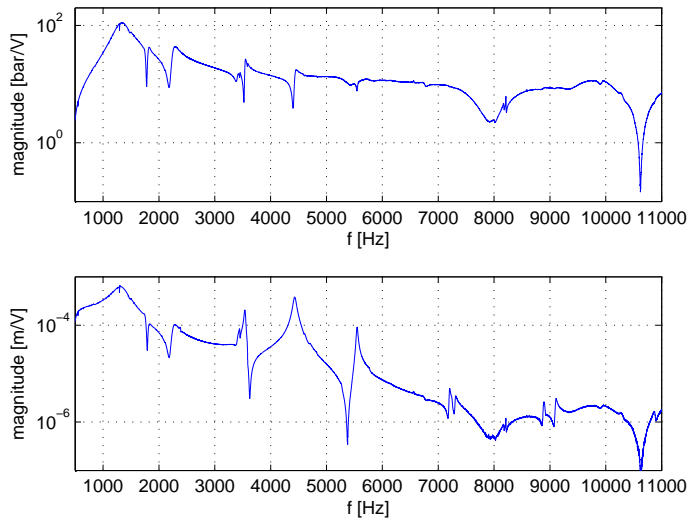


Figure 5: Frequency response function (FRF) from excitation voltage to dynamic pressure (upper plot) and to displacement at hose end (lower plot).

By this approach, the characteristics of different wave modes (e.g. phase and group velocities) of the waveguide are obtained, even though only one pipe segment is modeled and analyzed. This is achieved by the application of periodicity conditions in the direction of wave propagation. Moreover, a dynamic condensation of the three-dimensional pipe segment on the component interfaces is needed. Thus, the waveguide FEM can be seen as a quite efficient dynamic substructuring technique. The pressure field of a typical fluid mode of an assembled corrugated pipe is illustrated in Fig. 6. It is worth noting that the fluid wave speed is considerably altered due to the interaction with the corrugated pipe structure.

### 3.3 *Vibroacoustic Analysis of an Exhaust System*

In this section, pressure-induced vibrations of a production series rear muffler as depicted in Fig. 7 are investigated. For simplicity the inner structural parts of the rear muffler are removed. The periodically blown out exhaust gas leads to pressure pulsation within the exhaust system. These pulsations excite structural vibrations, which then additionally contribute to the sound radiation of the system. It is reported that this so-called surface radiated noise might dominate the noise radiated at the orifice [Brand, Garcia, and Wiemeler (2004); Brand and Wiemeler (2004a,b); Junge, Schube, and Gaul (2007)]. In this work, the focus is set on the pressure-induced vibrations and not on the sound radiation.

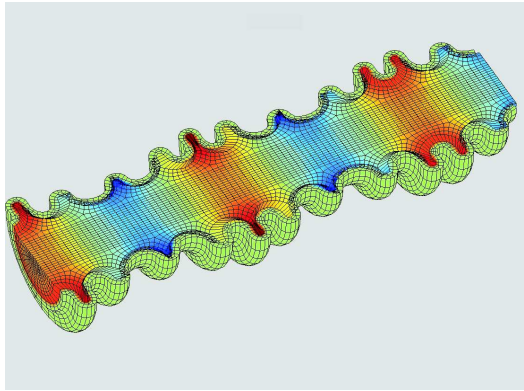


Figure 6: Illustration of fluid wave in a corrugated pipe.

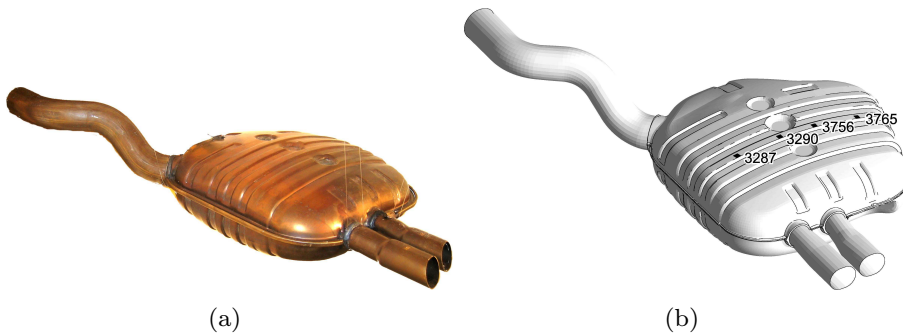


Figure 7: Picture of a production series rear muffler and corresponding CAE model. The system is depicted upside-down. The number on the right mark the location of the investigated nodes.

In order to quantify the pressure-induced vibrations of the rear muffler, the transfer function,  $H_{p \rightarrow u}$ , between the acoustic pressure at the inlet and the structural deflection at 4 locations on the surface is determined (cf. Fig. 7). The acoustic pressure at the inlet is measured by making use of the two-microphone-method [Seybert and Ross (1977)].

For the simulation a finite element model is set up with 179808 structural DOFs and 143602 fluid DOFs. For an efficient simulation a reduced model is computed as described in Section 2.3. The Rubin method is applied for the structural domain. The modal damping values obtained from an experimental modal analysis are incorporated in the damping matrix. The Craig-Bampton method is employed for the fluid domain. For each domain, 40 free-interface and fixed-interface nor-

mal modes are retained, respectively. The interface DOFs on the inlet and outlets sum up to 444 structural DOFs and 211 fluid DOFs yielding the same number of constraint modes and attachment modes, respectively. It is worth noting, that the interior acoustic fluid intersect with the surrounding fluid at the orifices. Previous investigation showed, that a radiation impedance condition approximates sufficiently accurate the occurring interaction at this cross-section [Levine and Schwinger (1948)]. The impedance condition yields complex entries in the damping matrix  $D_a$  [Gaul, Brunner, and Junge (2008)]. For the frequency sweep computations between 300 Hz and 600 Hz (with a step size of 1 Hz) the reduced-order models clearly outperform the full-order solution. A speedup of approximately factor 100 is obtained.

The plots in Fig. 8 show a comparison between the experimental (solid, black line) and simulative results (dashed, blue line). Each subplot represents the magnitude of the transfer function  $H_{p \rightarrow u}$  for one node on the surface of the rear muffler as depicted in Fig. 7. A strong excitability via the acoustic path is observed for all points –  $H_{p \rightarrow u}$  spans more than four orders of magnitude within the depicted frequency range between 300 Hz and 600 Hz. A comparison of the eigenfrequencies with the results of an experimental modal analysis reveals that the resonance frequencies are reached at eigenfrequencies of the structure. This explains the fact that the surface radiated noise shows a strongly tonal characteristic. All four subplots show a good agreement between experiments and simulations. It is worth noting, that the simulation is capable to predict the transfer function both qualitatively and quantitatively. The proposed method is thus suitable to efficiently predict pressure-induced vibrations in an early development stage and is capable to prevent cost-intensive modifications and time-consuming experiments.

#### 4 Conclusion

The Craig-Bampton and the Rubin method are successfully applied to acoustic fluid-structure coupled systems in order to achieve moderate computation times and moderate computer memory. The hydro- and vibroacoustic response of two automotive applications is analyzed in this research showing the applicability of the described component mode synthesis. For heavy fluid-structure coupling as in the case of fuel and brake pipes, the fluid and the structural partition need to be fully coupled to compute the corresponding component modes and to capture the strong interaction between the fluid and the flexible pipe shell. For light acoustic fluid-structure coupling as in the case of an exhaust system, uncoupled component modes of both the acoustic and the structural domain can be used to compute a reduced model. The results of the numerical simulation are compared to dynamic measurements. Good agreement is achieved with respect to hydro- and vibroacoustic

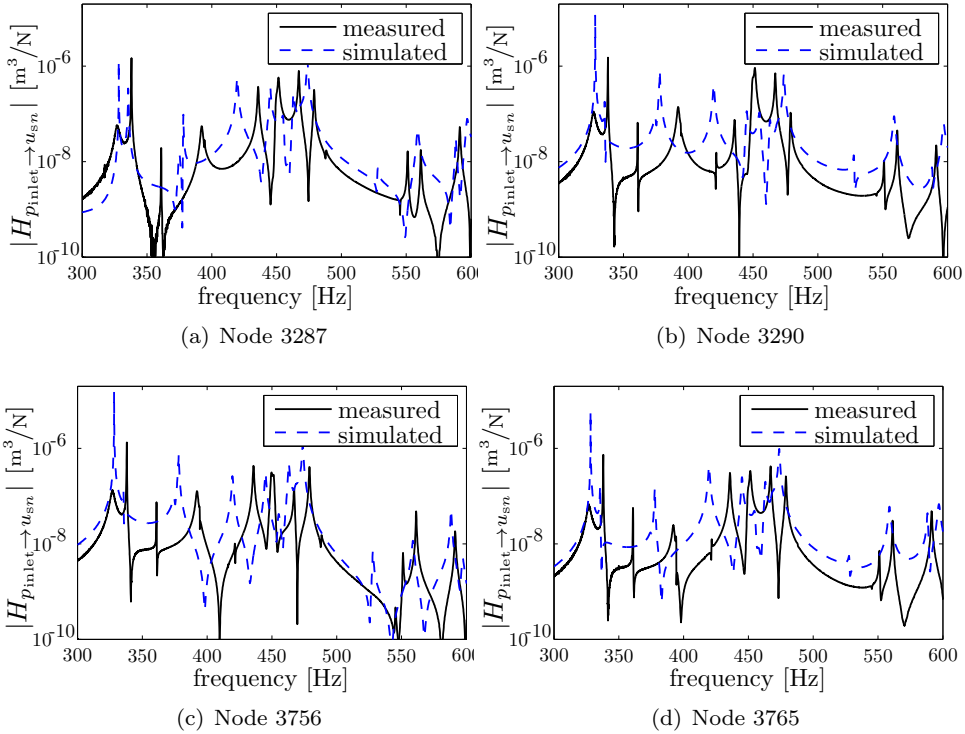


Figure 8: Pressure-induced structural vibrations. Comparison of experimental and simulative results.

transfer functions of complex fluid-structure coupled systems. Since the described modeling approach leads to moderate computation times, it is now possible to solve vibroacoustic optimization problems where multiple pipe configurations need to be evaluated. Moreover, the waveguide finite element method shows high potential to efficiently analyze wave properties of complex vibroacoustic waveguides with periodic properties in the direction of wave propagation.

**Acknowledgement:** The authors gratefully acknowledge the funding of this project by the German Research Society DFG in the transfer unit TFB 51 and by the Friedrich-und-Elisabeth-Boysen-Stiftung. Special thanks go to Dr. Karl Bendel from Robert Bosch GmbH for his help with the experimental setup. Moreover, the authors want to thank Dr.-Ing. Matthias Maess for his help and advice concerning model reduction topics and Dr.-Ing Stefan Engelke for his help with the experimental analysis of the investigated corrugated pipe.

## References

- Bobillot, A.; Balmès, E.** (2002): Iterative technique for eigenvalue solutions of damped structures coupled with fluids. *AIAA 43. Structures, Structural Dynamics, and Materials Conference*, vol. 168, pp. 1–9.
- Brand, J.-F.; Garcia, P.; Wiemeler, D.** (2004): Surface radiated noise of exhaust systems - calculation and optimization with CAE. In *Proceedings of the SAE 2004 World Congress & Exhibition*, volume 01.
- Brand, J.-F.; Wiemeler, D.** (2004): Surface radiated noise of exhaust systems – structural transmission loss test rig, part 1. In *Proceedings of the CFA/DAGA, Strasbourg*.
- Brand, J.-F.; Wiemeler, D.** (2004): Surface radiated noise of exhaust systems – structural transmission loss test rig, part 2. In *Proceedings of the ISMA*.
- Brunner, D.; Junge, M.; Gaul, L.** (2009): A comparison of fe-be coupling schemes for large scale problems with fluid-structure interaction. *International Journal for Numerical Methods in Engineering*, vol. 77, pp. 664–688.
- Craig, R. R.; Bampton, M. C. C.** (1968): Coupling of substructures for dynamic analysis. *AIAA Journal*, vol. 6, pp. 1313–1319.
- Craig Jr., R. R.** (2000): Coupling of substructures for dynamic analyses: An overview. In *Proceedings of the AIAA Dynamics Specialists Conference, Atlanta, GA*. Paper No. 2000-1573.
- de Klerk, D.; Rixen, D. J.; Voormeeren, S. N.** (2008): General framework for dynamic substructuring: History, review, and classification of techniques. *AIAA Journal*, vol. 46, pp. 1169–1181.
- Everstine, G. C.** (1981): A symmetric potential formulation for fluid-structure interaction. *Journal of Sound and Vibration*, vol. 79, pp. 157–160.
- Felippa, C. A.** (1985): Symmetrization of the contained compressible-fluid vibration eigenproblem. *Communications in Applied Numerical Methods*, vol. 1, pp. 241–247.
- Gaul, L.; Brunner, D.; Junge, M.** (2008): Coupling a fast boundary element method with a finite element formulation for fluid-structure interaction. In Marburg, S.; Nolte, B.(Eds): *Computational Acoustics of Noise Propagation in Fluids*. Springer, Berlin Heidelberg.
- Gaul, L.; Kögel, M.; Wagner, M.** (2003): *Boundary Element Methods for Engineers and Scientists*. Springer, Berlin.
- Guyan, R. J.** (1965): Reduction of stiffness and mass matrices. *AIAA Journal*, vol. 3, pp. 380.

- Herrmann, J.** (2011): *Hydro- and Vibroacoustic Analysis of Piping Systems Using Efficient Substructuring and Dynamic Measurements*. Ph.D. thesis, Institute of Applied and Experimental Mechanics, University of Stuttgart, 2011.
- Herrmann, J.; Haag, T.; Gaul, L.; Bendel, K.; Horst, H. G.** (2008): Experimentelle Untersuchung der Hydroakustik in Kfz-Leitungssystemen. In *Proc. of DAGA*, Dresden.
- Herrmann, J.; Koreck, J.; Maess, M.; Gaul, L.; von Estorff, O.** (2011): Frequency-dependent damping model for the hydroacoustic finite element analysis of fluid-filled pipes with diameter changes. *Mechanical Systems and Signal Processing*, vol. 25, pp. 981–990.
- Herrmann, J.; Maess, M.; Gaul, L.** (2010): Substructuring including interface reduction for the efficient vibro-acoustic simulation of fluid-filled piping systems. *Mechanical Systems and Signal Processing*, vol. 24, pp. 153–163.
- Junge, M.** (2010): *Model Reduction Methods for FE-BE Coupling Applied to Vibro-Acoustic Simulations and Experimental Validation*. Ph.D. thesis, Institute of Applied and Experimental Mechanics, University of Stuttgart, 2010.
- Junge, M.; Brunner, D.; Becker, J.; Gaul, L.** (2009): Interface reduction for the Craig-Bampton and Rubin method applied to FE-BE coupling with a large fluid-structure interface. *International Journal for Numerical Methods in Engineering*, vol. 77, pp. 1731–1752.
- Junge, M.; Brunner, D.; Walz, N.; Gaul, L.** (2010): Simulative and experimental investigations on pressure-induced structural vibrations of a rear muffler. *Journal of the Acoustical Society of America*, vol. 128, pp. 2782–2791.
- Junge, M.; Schube, F.; Gaul, L.** (2007): Sound Radiation of an Expansion Chamber due to Pressure Induced Structural Vibrations. In *Proc. of DAGA*, Stuttgart.
- Levine, H.; Schwinger, J.** (1948): On the radiation of sound from an unflanged circular pipe. *Physical Review*, vol. 73, no. 4, pp. 383 – 406.
- Mace, B.; Duhamel, D.; Brennan, M.; Hinke, L.** (2005): Wave number prediction using finite element analysis. *Journal of the Acoustical Society of America*, vol. 117, pp. 2835–2843.
- Maess, M.** (2006): *Methods for Efficient Acoustic-Structure Simulation of Piping Systems*. Ph.D. thesis, Institute of Applied and Experimental Mechanics, University of Stuttgart, 2006.
- Maess, M.; Gaul, L.** (2006): Substructuring and model reduction of pipe components interacting with acoustic fluids. *Mechanical Systems and Signal Processing*, vol. 20, pp. 45–64.

**Maess, M.; Herrmann, J.; Gaul, L.** (2007): Finite element analysis of guided waves in fluid-filled corrugated pipes. *Journal of the Acoustical Society of America*, vol. 121, pp. 1313–1323.

**Ohayon, R.** (2004): Reduced models for fluid-structure interaction problems. *International Journal for Numerical Methods in Engineering*, vol. 60, pp. 139–152.

**Rixen, D.** (2004): A dual Craig-Bampton method for dynamic substructuring. *Journal of Computational and Applied Mathematics*, vol. 168, pp. 383–391.

**Rubin, S.** (1975): Improved component-mode representation for structural dynamic analysis. *AIAA Journal*, vol. 13, pp. 995–1006.

**Seybert, A. F.; Ross, D. F.** (1977): Experimental determination of acoustic properties using a two-microphone random-excitation technique. *Journal of the Acoustical Society of America*, vol. 61, no. 5, pp. 1362 – 1370.

**Tijdeman, H.** (1975): On the propagation of sound waves in cylindrical tubes. *Journal of Sound and Vibration*, vol. 39, pp. 1–33.

**Zienkiewicz, O.; Taylor, R.** (2000): *The Finite Element Method*. Butterworth-Heinemann, Oxford.